ELSEVIER

Surface and Coatings Technology 160 (2002) 177–186

SURFACE & COATINGS TECHNOLOGY

www.elsevier.com/locate/surfcoat

A new model for the computation of the composite hardness of coated systems

E.S. Puchi-Cabrera*

School of Metallurgical Engineering and Materials Science, Faculty of Engineering, Universidad Central de Venezuela, Apartado Postal 47885, Los Chaguaramos, Caracas1045, Venezuela

Received 31 January 2002; accepted in revised form 12 June 2002

Abstract

The present communication proposes a new model for the computation of the composite hardness of coated systems as a function of the relative indentation depth, the hardness of both coating and substrate and two material constants that characterize the performance of the film during the indentation test. The model is developed from several important considerations which can be summarized as follows: (1) The substrate starts to contribute to the composite hardness at penetration depths of the order of 0.07–0.2 times the coating thickness, as suggested in the literature. (2) Above such a boundary the composite hardness depends mainly on the intrinsic hardness of the coating, whereas below it such a hardness is determined essentially by the hardness of the mixture that encompasses the remaining part of the film and the plastically deformed substrate material. (3) The hardness of such a mixture is assumed to be constant, except for the possible indentation size effect that could be displayed by the substrate. (4) The composite hardness is given by a linear law of mixtures in terms of the hardness of the coating and such a mixture, and the volume fraction of both materials under the indenter, at any given depth of the latter. It is shown that the model proposed describes very well the hardness data obtained in different systems including: Ti and TiC formed on a chromium steel of a high carbon content; TiN; TiCN and CrN deposited on M2 steel; and $TiN_{0.55}$, $TiN_{0.65}$, $TiN_{0.75}$, $ZrN_{0.50}$, $ZrN_{0.60}$ and $ZrN_{0.70}$ deposited on 316L stainless steel substrate. The results are also compared with those derived from the models earlier advanced by Jönsson and Hogmark, Burnett and Rickerby, Chicot and Lesage and Tuck et al., without taking into consideration the indentation size effect of the film. It is shown that the modified version of the earlier model put forward by Korsunsky et al., published recently by Tuck et al., constitutes a particular form of the model here proposed.

Keywords: Modeling; Composite hardness; Relative indentation depth; Indentation diagonal

1. Introduction

The optimization of deposition processes employed in the synthesis of thin hard coatings used in many industrial applications has led to development of different experimental techniques for the characterization of such complex systems. Particular attention has been paid to the evaluation of the way in which such systems respond to contact loads, by means of simple, non-destructive techniques that could be put in practice in standard industrial laboratories. Among these, micro and macro indentation tests play a fundamental role since they could be very efficient in the evaluation of the mechanical response of a film–substrate system to contact stresses, which makes them a very useful and cost-effective tool in the process of selection and optimization of coatings for particular applications. However, the interpretation of the indentation data obtained from coated systems could be very complex due to different reasons. Firstly, the fact that the response of the system depends significantly on the scale of contact, being dominated by the film hardness at small scales in comparison with the coating thickness and by the substrate hardness at large scales. Secondly, the observation

*Tel.: +58-212-6628927; fax: +58-212-7539017.
E-mail address: epuchi@reacciun.ve (E.S. Puchi-Cabrera).

0257-8972/02/$ - see front matter © 2002 Elsevier Science B.V. All rights reserved.
PII: S0257-8972(02)00394-8

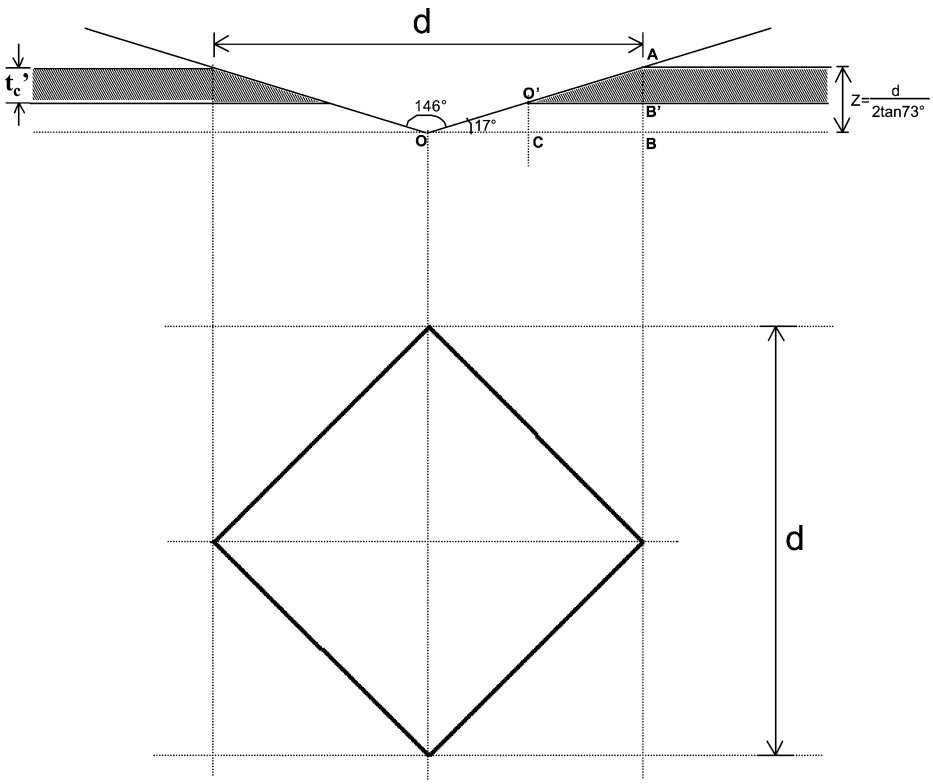

Fig. 1. Schematic drawing of the cross-section and top view of the indentation process of a coated material.

that both the film and substrate hardness themselves could also dependent on the scale of contact, giving rise to an indentation size effect (ISE) in both materials. Thus, in order to determine the hardness of both mono- and multilayer thin films from standard indentation tests a number of models have been developed in the past few years [1–17]. More recently, an investigation has been carried out [18] in order to modify some of the classical models available, in particular those advanced by Jönsson and Hogmark [2], Burnett and Rickerby [5,6], Chicot and Lesage [10] and Korsunsky et al. [13], by incorporating the ISE of both the substrate and film through the power relationship proposed by Meyer, for the description of the change in hardness with the indentation diagonal. In this latter study, a numerical least square non-linear regression algorithm was also outlined in order to compute the constants involved in any of the modified models. Thus, the present investigation has been conducted in order to develop on a rational basis and from simple geometrical considerations, a different model capable of capturing the essential features of the complexity of the indentation process of a coated systems and also of describing accurately that change in the composite hardness of a coating–substrate system as a function of the indentation size, the latter employed as a measured of the scale of indentation during the test.

2. Details of the model proposed

Fig. 1 illustrates schematically a cross-section and a top view of the indentation of a coated substrate employing a Vickers indenter. In this figure, d represents the indent diagonal and z the indent depth. For the Vickers indenter the angle between opposite edges is 146°, whereas that between opposite faces is 136°. The model proposed here considers as a first approximation that, according to Fig. 1, the contribution of the substrate to the composite hardness takes place as soon as the indenter crosses the boundary defined as t'_c, determined by some fraction, f, of the film thickness and not the coating thickness itself, t_c. Hence, as it is shown in the above Figure, $t'_c = ft_c$.

Therefore, above this boundary the composite hardness, H, depends mainly on the hardness of the coating whereas below it H would be determined by the hardness of the mixture that encompasses the remaining part of the coating and the plastically deformed substrate underneath the film. In the forthcoming, this mixture will be described as the ‘substrate’ and it is further assumed that its intrinsic hardness is approximately constant, except for the indentation size effect that could be displayed by the actual substrate material. The justification behind such assumptions will be discussed in detail in Section 4.

Also, due to symmetric considerations it is possible to concentrate only on the right-hand side of the drawing. Thus, the total area of the system under the indenter, A_T, can be represented by the triangle OAB, whose area is given by:

$$\text{Area of OAB} = \frac{1}{2}\text{OB}\bullet\text{AB} = \frac{z^2\tan 73^\circ}{2} \tag{1}$$

Similarly, the area entirely under the coating, A_C, is represented by the area of the triangle O′AB′:

$$\text{Area of O}'\text{A}'\text{B} = \frac{1}{2}\text{O}'\text{B}'\bullet\text{A}'\text{B}' = \frac{t_c'^2}{2\ \tan\ 17^\circ} \tag{2}$$

Thus, the area of the 'substrate' material under the indenter, A_S, is simply given by the difference:

$$A_s = \frac{1}{2}\left(z^2\tan 73^\circ - \frac{t_c'^2}{\tan\ 17^\circ}\right) \tag{3}$$

Considering the equivalence between the volume and area fractions, the volume fraction of the 'substrate' material under the indenter, X_S, is given by:

$$X_s = \frac{A_s}{A_T} = \frac{z^2 - \dfrac{t_c'^2}{\tan\ 17^\circ\ \tan\ 73^\circ}}{z^2} = \frac{z^2 - \alpha}{z^2} \quad \text{and} \quad \alpha = \frac{t_c'^2}{\tan\ 17^\circ\ \tan\ 73^\circ} \tag{4}$$

Also, the volume fraction of the coating under the indenter, X_C, is given by:

$$X_C = \frac{t_c'^2}{z^2\ \tan\ 17^\circ\ \tan\ 73^\circ} = \frac{\alpha}{z^2} \tag{5}$$

Thus, the rate of change of the 'substrate' fraction as the indenter penetrates the system is simply given by:

$$\frac{dX_S}{dz} = \frac{2\alpha}{z^3} = 2\bullet\ \frac{\alpha}{z^2}\ \bullet\frac{1}{z} = 2X_C\ z^{-1} \tag{6}$$

As it will be discussed in Section 4, this result could be generalized by considering that:

$$\frac{dX_S}{dz} = 2X_C z^{n'} \quad \text{with} \quad -3 \le n' \le -1 \tag{7a}$$

However, for convenience, the above expression could be modified further by assuming that:

$$n' = n - 1 \quad \text{with} \quad -2 \le n \le 0 \tag{7b}$$

leading to the following expression:

$$\frac{dX_S}{dz} = 2X_C z^{n-1} \tag{7c}$$

The integration of the above expression yields a general equation for the change in the substrate fraction with the indenter stroke:

$$\int_0^{X_s}\frac{dX_S}{X_C} = \int_0^{X_s}\frac{dX_S}{1-X_S} = 2\int_0^{z} z^{n-1}dz \tag{8}$$

That is to say:

$$-\ln(1-X_S) = \frac{2z^n}{n} = k'z^n \quad \text{where} \quad k' = \frac{2}{n}$$

from which the following equation is obtained:

$$X_S = 1 - \exp(-k'z^n) = 1 - \exp\left[-k't_c^n\left(\frac{z}{t_c}\right)^n\right] \tag{9}$$

which can also be expressed in terms of the relative indentation depth, $Z_R = z/t_c = d/7t_c$ as:

$$X_S = 1 - \exp(-kZ_R^n) \quad \text{where} \quad k = k't_c^n \tag{10}$$

Assuming that the composite hardness, H, is given by a simple law of mixtures in terms of the volume fractions of coating and 'substrate' and their hardness, H_C and H_S, respectively, as suggested by Bückle [1]:

$$H = H_S\bullet X_S + H_C\bullet X_C \tag{11}$$

expression which combined with the previous equation yields a formulation for the computation of the composite hardness according to the present model:

$$H = H_S + (H_C - H_S)\exp(-kZ_R^n) \tag{12}$$

where the constants k and n represent material parameters that characterize the change in hardness as the indenter passes from the coating to the substrate and therefore constitute an important feature of the film-substrate system.

3. Experimental procedure

The new model here advanced was tested employing different data sets. Firstly, the data published earlier by Chicot et al. [14] for Ti and TiC films formed on a steel substrate of the following composition (wt.%): 1.2 C, 1 Cr. According to these authors, the pure Ti film, of 4 μm in thickness, was deposited by magnetron sputtering under an argon atmosphere and a pressure of 3×10^{-3} mbar. Subsequently, the transformation of the Ti film into TiC occurred during the annealing of the samples in the temperature range of 700–1100 °C for 1 h. On the basis of X-ray diffraction analysis conducted with the treated samples, it was reported, that the complete transformation of the Ti deposit took place at 1100 °C, giving rise to an homogeneous TiC film of the same thickness as the initial Ti coating. The hardness data was determined employing a Vickers indenter and loads in the range of 0.1–10 N. The values reported, corresponded to a mean of five indentation for each load.

The second set of data involved a number of standard coated samples produced by filtered cathodic arc at UES Arcomat, Inc. In this case, polished discs of 19 mm in diameter and 5 mm thick of a M2 tool steel were

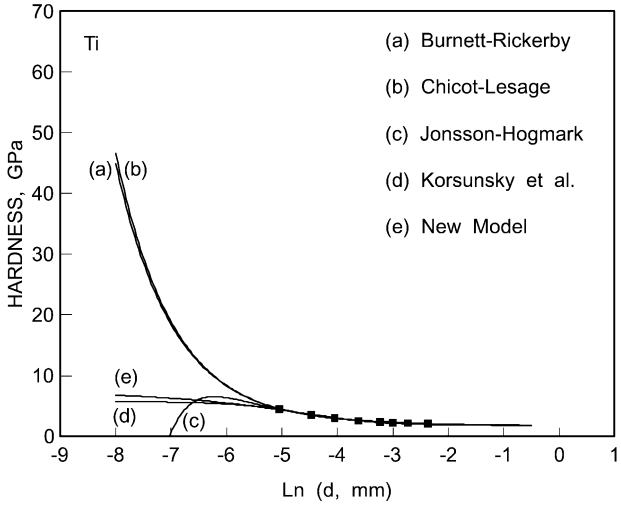

Fig. 2. Change in hardness with indentation diagonal for a Ti film of 4 μm in thickness, deposited on a Cr steel substrate.

cleaned ultrasonically in acetone and isopropyl alcohol and subsequently coated in the LAFAD™ system at UES Inc, Dayton, OH, USA with CrN, TiN and TiCN films, whose thickness varied between approximately 1 and 4 μm. Prior to the introduction of gases such as argon, nitrogen and methane, the deposition chamber was evacuated at a pressure of 7×10^{-4} Pa. TiN and CrN were deposited employing Ti and Zr cathodes, respectively, in filtered arc mode in nitrogen atmosphere. The TiCN film was deposited employing Ti cathodes in a mixed atmosphere of nitrogen and methane. The hardness data for the CrN and TiCN coatings were obtained employing loads in the range of approximately 0.15–9.8 N, whereas those for the TiN film were obtained with loads in the range of approximately 0.25–9.8 N.

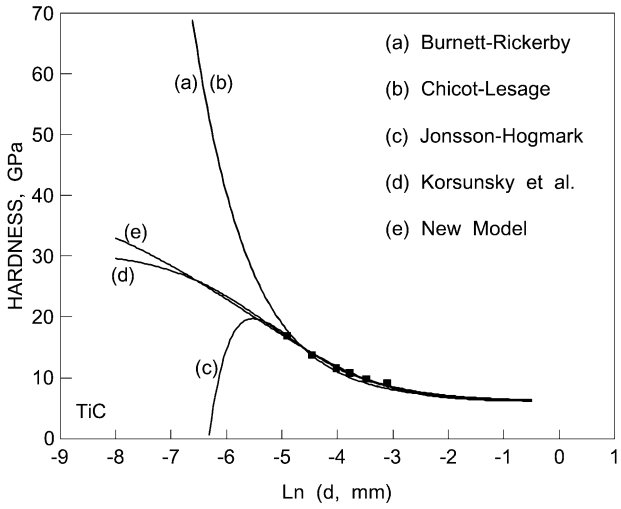

Fig. 3. Change in hardness with indentation diagonal for a TiC film of 4 μm in thickness, deposited on a Cr steel substrate.

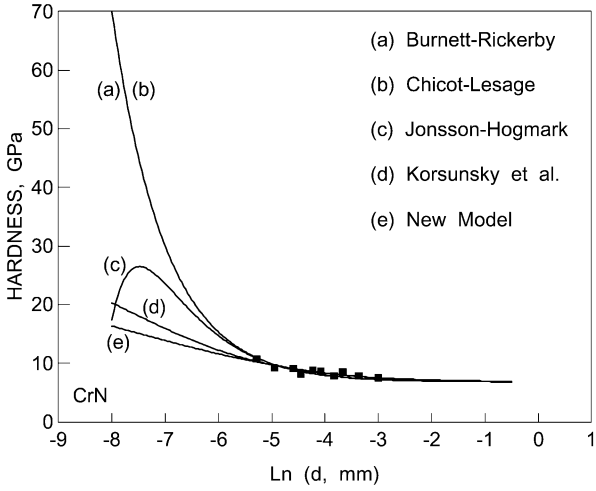

Fig. 4. Change in hardness with indentation diagonal for a CrN film of 1.12 μm in thickness, deposited on a M-2 steel substrate.

On the other hand, in the present work, a number of samples of 316L stainless steel with a cylindrical shape, were polished mechanically to a specular finish and coated industrially by unbalanced magnetron sputtering at Teer Coatings, Hartlebury, UK, with TiN_x and ZrN_y deposits of three different stoichiometries: $TiN_{0.55}$; $TiN_{0.65}$; $TiN_{0.75}$; $ZrN_{0.50}$; $ZrN_{0.60}$; and $ZrN_{0.70}$. All these coatings had a mean thickness of approximately 3 μm. Vickers hardness tests were conducted on such samples, employing loads of 0.049, 0.098, 0.245, 0.49, 0.98, 1.96 and 3.92 N. At least 12 measurements were conducted for each load applied. SEM techniques after proper calibration, were also employed in order to evaluate the indentation size produced at the lowest loads used and the possible occurrence of fracture in the coating under these testing conditions.

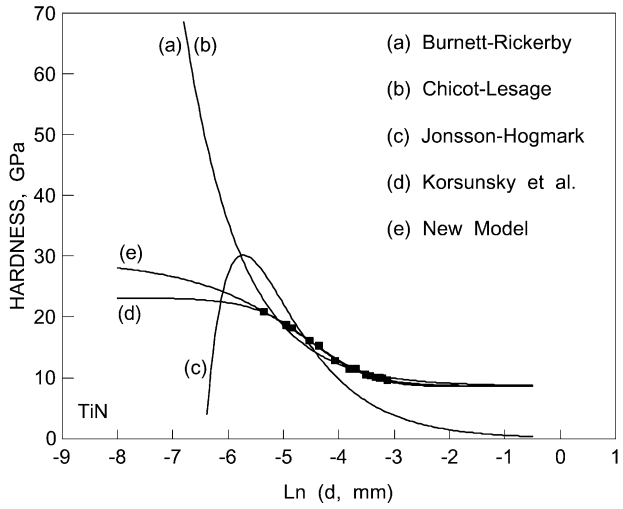

Fig. 5. Change in hardness with indentation diagonal for a TiN film of 3.25 μm in thickness, deposited on a M-2 steel substrate.

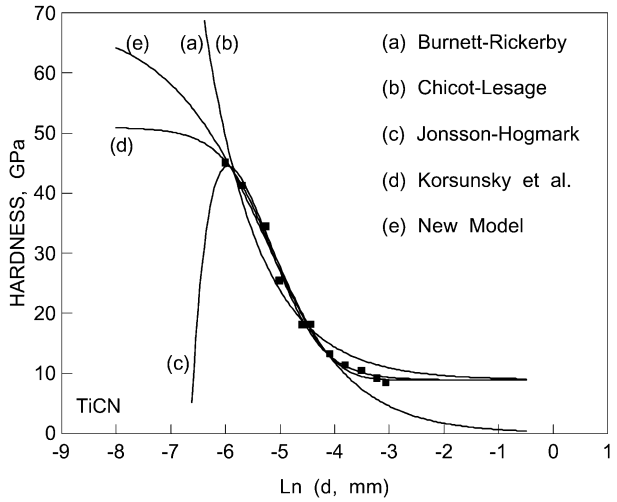

Fig. 6. Change in hardness with indentation diagonal for a TiCN film of 3.25 μm in thickness, deposited on a M-2 steel substrate.

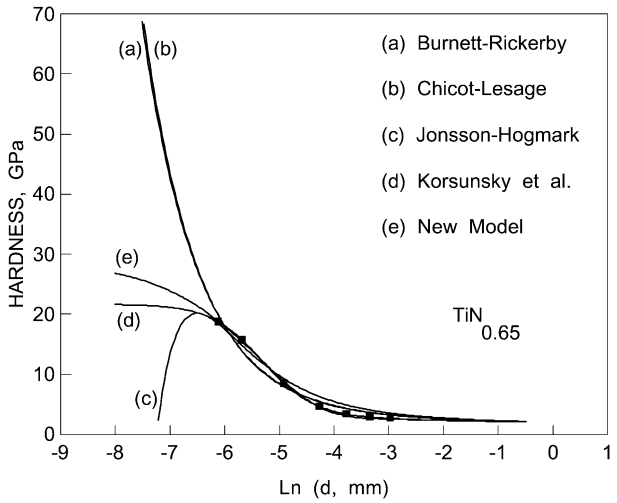

Fig. 8. Change in hardness with indentation diagonal for a $TiN_{0.65}$ film of 3 μm in thickness, deposited on a 316L stainless steel substrate.

4. Results and discussion

Figs. 2–12 illustrate, as solid points, the change in the composite hardness as a function of the logarithm of the indentation diagonal in μm and, as solid lines, the description of the experimental data by means of four well known models reported in the literature, and the new model proposed in the present work. The numerical results corresponding to the different models applied, for each of the coatings analyzed, are reported in Tables 1 and 2. The first two models analyzed were those advanced by Burnett and Rickerby [5,6] and Chicot and Lesage [10] for which the composite hardness as function of the indentation diagonal, without taking into consideration the indentation size effect of the coating, is given by the following relationships:

$$H_C = H_S + 3(H_F - H_S)\left(\frac{H_F}{E_F}\right)^{1/2}\frac{t_c}{d}\tan^{1/3}\xi \qquad (13)$$

and

$$H_C = H_S + \left\{\frac{3t_c}{2d} \times \left[\left(\frac{H_F}{E_F}\right)^{1/2} + \left(\frac{H_S}{E_S}\right)^{1/2}\right]\tan^{1/3}\xi\right\}(H_F - H_S), \qquad (14)$$

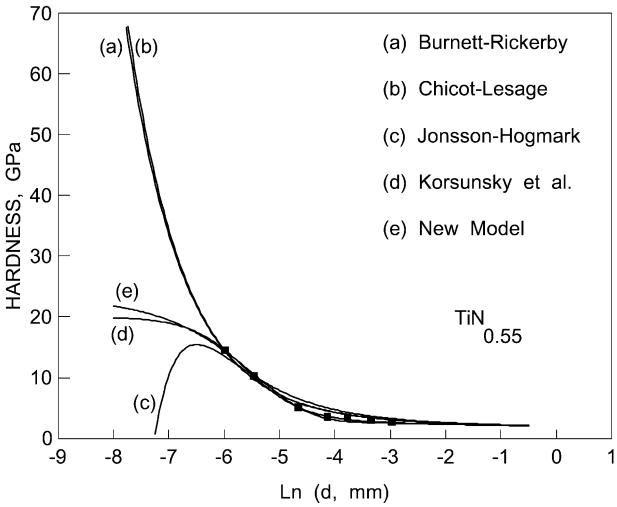

Fig. 7. Change in hardness with indentation diagonal for a $TiN_{0.55}$ film of 3 μm in thickness, deposited on a 316L stainless steel substrate.

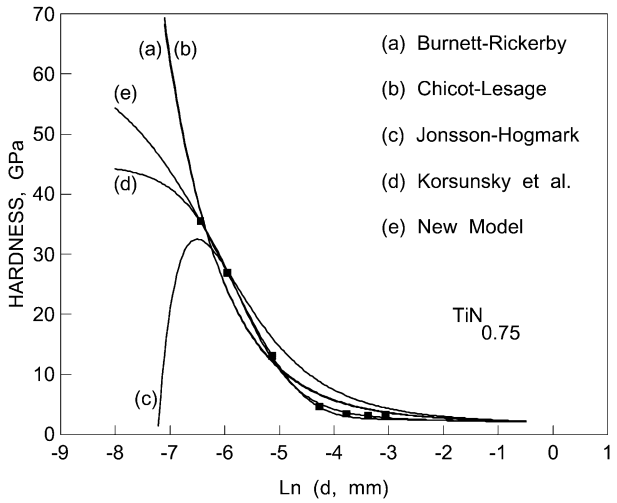

Fig. 9. Change in hardness with indentation diagonal for a $TiN_{0.75}$ film of 3 μm in thickness, deposited on a 316L stainless steel substrate.

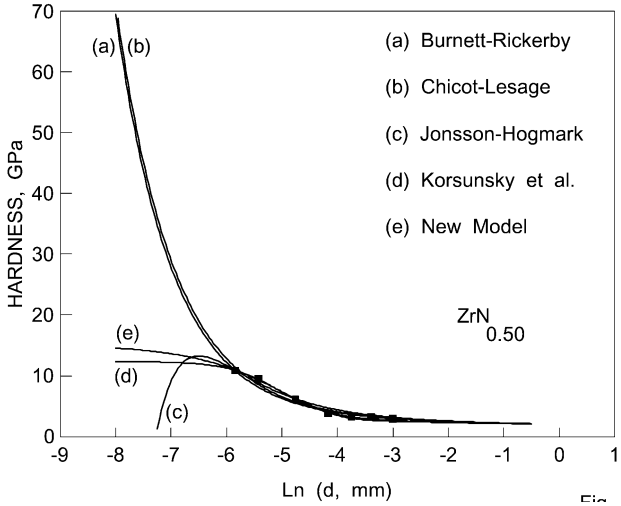

Fig. 10. Change in hardness with indentation diagonal for a $ZrN_{0.50}$ film of 3 μm in thickness, deposited on a 316L stainless steel substrate.

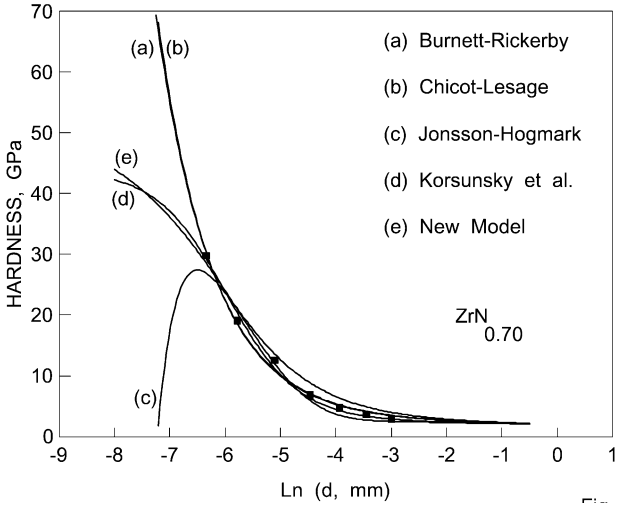

Fig. 12. Change in hardness with indentation diagonal for a $ZrN_{0.70}$ film of 3 μm in thickness, deposited on a 316L stainless steel substrate.

respectively. In the above expressions, E_F and E_S represent the Young's modulus of the film and substrate, respectively, and ξ the indenter semi-angle (73°). As it is shown in Table 1 the Chicot–Lesage model predicts values for the film hardness somewhat greater than those obtained from the Burnett–Rickerby model. However, as it is shown in the figures mentioned before, both models provide virtually the same description of the experimental data and even in some cases it is not possible to distinguish between the descriptive curves predicted by each model.

The third model employed in the analysis was that advanced by Jönsson and Hogmark [2], according to which the composite hardness is given by:

$$H_c = H_S + \left[2C\frac{t_c}{d} - \left(C\frac{t_c}{d}\right)^2\right](H_F - H_S) \quad (15)$$

where the constant C can take a value between 0.5 and 1, depending on whether the coating tends to fracture or to deform plastically during the indentation. Figs. 2–12 illustrate clearly that this approach, although gives rise to a relatively satisfactory description of the experimental data, it breaks down at indentation diagonal values lower than those measured experimentally, obviously due the polynomial form that is prescribed for the expression of the coating fraction under the indenter.

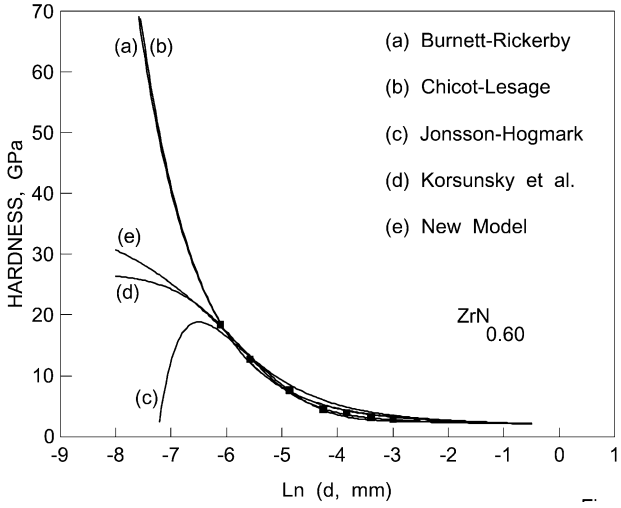

Fig. 11. Change in hardness with indentation diagonal for a $ZrN_{0.60}$ film of 3 μm in thickness, deposited on a 316L stainless steel substrate.

Table 1
Values of the parameters involved in the models advanced by Burnett and Rickerby [5,6], Chicot and Lesage [10] and Jönsson and Hogmark [2], for the different materials analyzed

Material	Hardness model						
	Burnett–Rickerby		Chicot–Lesage		Jönsson–Hogmark		
	H_S, GPa	r^2	H_S, GPa	r^2	H_S, GPa	C	r^2
Ti	5.95	0.996	7.08	0.996	6.56	0.50	0.993
TiC	25.6	0.956	28.0	0.955	19.7	1.00	0.991
CrN	20.4	0.845	23.3	0.845	26.5	0.50	0.848
TiN	29.1	0.949	29.8	0.949	30.2	1.00	0.768
TiCN	36.5	0.947	38.5	0.947	44.5	0.80	0.976
$TiN_{0.55}$	15.8	0.977	17.3	0.980	15.5	0.50	0.931
$TiN_{0.65}$	18.5	0.972	20.6	0.972	20.2	0.50	0.962
$TiN_{0.75}$	23.4	0.980	26.9	0.980	32.5	0.50	0.939
$ZrN_{0.50}$	14.4	0.970°	15.6	0.970	13.3	0.50	0.966
$ZrN_{0.60}$	17.8	0.993°	19.7	0.994	18.9	0.50	0.961
$ZrN_{0.70}$	21.6	0.993°	24.6	0.993	27.4	0.50	0.954

Table 2
Values of the parameters involved in the models advanced by Tuck et al. [15] and the present model

Material	Hardness model							
	Tuck et al.				Present model			
	H_S, GPa	k	n	r^2	H_S, GPa	k	n	r^2
Ti	5.75	5.98	1.61	0.996	7.29	2.24	0.68	0.987
TiC	30.9	5.59	1.04	0.992	44.7	2.32	0.42	0.983
CrN	31.0	7.99	0.73	0.843	33.7	2.30	0.25	0.824
TiN	23.2	3.85	1.88	0.998	29.3	1.88	0.82	0.996
TiCN	51.0	18.3	2.15	0.994	68.8	3.57	0.90	0.992
$TiN_{0.55}$	20.0	31.8	1.97	0.999	31.3	4.55	0.75	0.996
$TiN_{0.65}$	21.7	21.9	2.11	0.999	29.0	3.89	0.91	0.997
$TiN_{0.75}$	44.8	36.1	1.87	0.999	65.0	4.90	0.78	0.999
$ZrN_{0.50}$	12.3	13.2	2.15	0.996	16.9	3.16	0.86	0.992
$ZrN_{0.60}$	27.0	24.3	1.66	0.998	37.3	4.04	0.71	0.994
$ZrN_{0.70}$	43.8	28.1	1.57	0.993	52.2	4.38	0.76	0.987

Also, it is important to observe that the quality of the fit of the experimental data is not much better for this model than for the two previous ones, even though the composite hardness does not only depend on the film hardness but also on the constant C, which in the present case varied freely between the permissible values considered for this parameter.

The fourth model used in the present study was that published by Tuck et al. [15], which constitutes a refinement of the previous model advanced by Korsunsky et al. [13]. According to this new version of the model, the composite hardness is given as a function of the relative indentation depth ($Z_R = d/7t_c$) by an expression of the form:

$$H_c = H_S + \frac{H_F - H_S}{1 + kZ_R^X} \tag{16}$$

where both k and X represent a dimensionless hardness transition parameter and a power exponent, respectively, that depend on the deformation mode and geometry. Of the four models analyzed so far, this approach provides the best description since the composite hardness depends on three parameters that must be identified from the experimental data. Also, it predicts a smooth saturation of the composite hardness at low indentation diagonal values, towards the value corresponding to the film hardness. This behavior differs markedly from that predicted by the Burnett–Rickerby and Chicot–Lesage models for which the composite hardness tends to increase as the indentation diagonal decreases.

The new model advanced in the present communication is also observed to saturate at low values of the indentation diagonal, where the composite hardness tends to achieve the predicted value of the film hardness. However, it is also observed that, for most cases analyzed, the predicted value for the film hardness is somewhat higher than that predicted by the model proposed by Tuck et al. [15]. In the case of the CrN coating the reverse behavior can be seen, a trend that could be due to the particular set of hardness data available for this coating which rendered the lowest determination coefficient of all the materials analyzed. Also, in Table 2 it can be observed that the values of the constant k are lower in the new model in comparison with Tuck et al. model [15] and that the exponent n is in the range of approximately 0.4–0.9. In the model published by Tuck et al. [15] this exponent varies between approximately 1 and 3. The determination coefficients for both models are very similar, indicating a satisfactory description of the experimental data.

There are several important aspects that must be discussed regarding the model proposed. In the first place, the basic assumption on which it is based in the sense that the contribution of the substrate to the composite hardness starts to be effective before the indenter crosses the film thickness. Such a consideration is widely supported by the experimental data concerning the change in the composite hardness as a function of the indent diagonal. As it has been shown in Figs. 2–12, even at penetration depths lower than the coating thickness the composite hardness decreases significantly as the indentation diagonal increases.

If the substrate started contributing to the composite hardness just as the indenter crossed the coating–substrate interface, in the region where $d/7 < t_c$ the hardness should be almost constant and equal to the absolute hardness of the coating, except for the indentation size effect that could be displayed by the film. According to Jönsson and Hogmark [2] the fraction of the film thickness from which the substrate begins to contribute to the composite hardness varies between approximately 0.07 and 0.2, where the most unfavorable case is that of a hard coating on a softer substrate. Also, according to the data presented by Korsunsky et al. [13], this fraction could be of the order of 0.1 or less. Therefore, what in the present model has been considered to be the 'substrate' material under the indenter is indeed a mixture of the remaining part of the coating and plastically deformed substrate located underneath the film, in which the actual plastically deformed substrate fraction increases as the indenter stroke advances. However, Figs. 2–12 also illustrate that this extremely complex situation can still be modeled by means of a simplified approach that considers the composite hardness as the contribution of essentially two different materials: coating and 'substrate'.

Secondly, a close examination of Eq. (12) indicates that for small values of the term kZ_R^n, it reduces to Eq. (16), that is to say to the expression of the model proposed by Tuck et al. [15]. However, the more general Eq. (12) has been developed on the basis of a simple geometrical model rather than on the basis of the work of indentation, from which Eq. (16) was first developed

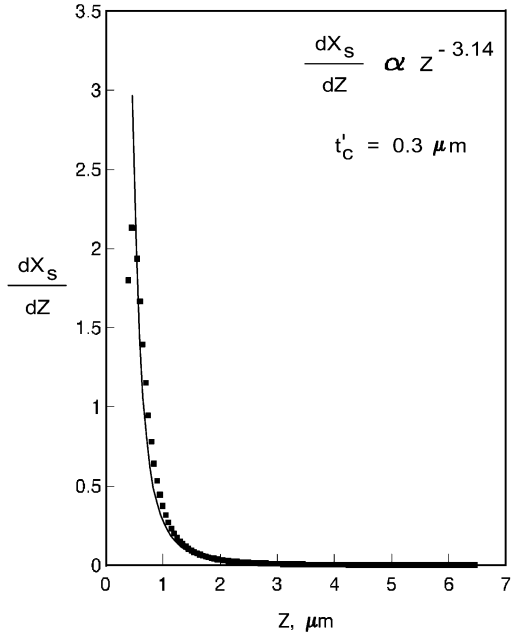

Fig. 13. Theoretical description (solid curve) of the variation in the rate of change of the substrate fraction with indentation depth, dX_S/dz, with indentation depth, z. The points have been computed assuming that the 'substrate' area under the indenter is given by Eq. (18).

by Korsunsky et al. [13]. It is important to point out that, in spite of the close relationship between Eq. (12) and Eq. (16), the simultaneous determination of the parameters H_F, k and n in both models from the experimental data by means of non-linear regression analysis, leads to different results.

Thirdly, the development of Eq. (12) stems from the critical supposition that Eq. (6) can be generalized by assuming that:

$$\frac{dX_S}{dz}\alpha z^{n-1} \quad \text{with } n \leq 0 \tag{17}$$

which in our opinion is justified given the ill definition of the exact area (volume) under the indenter that contributes to the composite hardness. Eq. (6) has been developed assuming that the total area of material under the indenter (coating and 'substrate') that contributes to such a hardness is that of the triangle OAB, which represents one of the limiting conditions. However, if it is assumed that the area of the 'substrate' material under the indenter that contributes to the composite hardness is that defined by the triangle OO′C, that is to say, only the area of the substrate that is in contact with the indenter, then:

$$A_S = \frac{1}{2}\left[z^2 \tan 73° - \frac{t'^2_c}{\tan 17°}\right](z - t'_c) \tag{18}$$

Fig. 13 illustrates that, in this case, assuming reasonable values for the parameter t'_c, the rate of change of the 'substrate' fraction with the indenter stroke can be described with a different dependence on z:

$$\frac{dX_S}{dz}\alpha z^{-3.14} \tag{19}$$

Thus, depending on the consideration of the area of both coating and 'substrate' under the indenter that contribute to the composite hardness the z dependence of dX_S/dz can vary approximately between -3 and -1, which justifies the assumption made regarding the development of equation 7c.

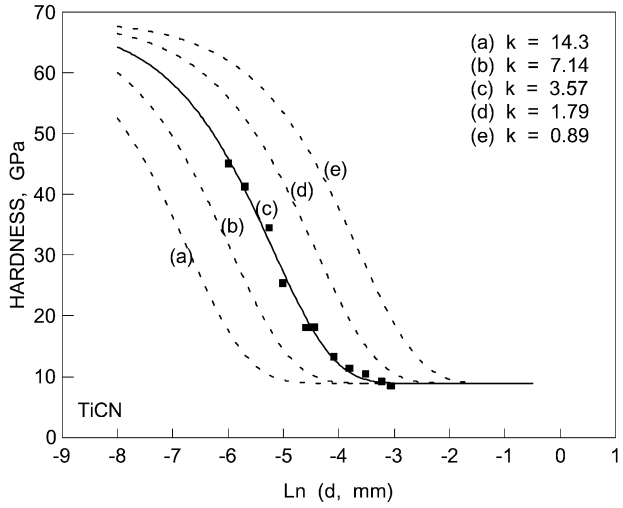

Fig. 14. Effect of the change in the parameter k in Eq. (12), on the displacement of the composite hardness of the TiCN curve. Both the film hardness and the parameter n have been kept constant.

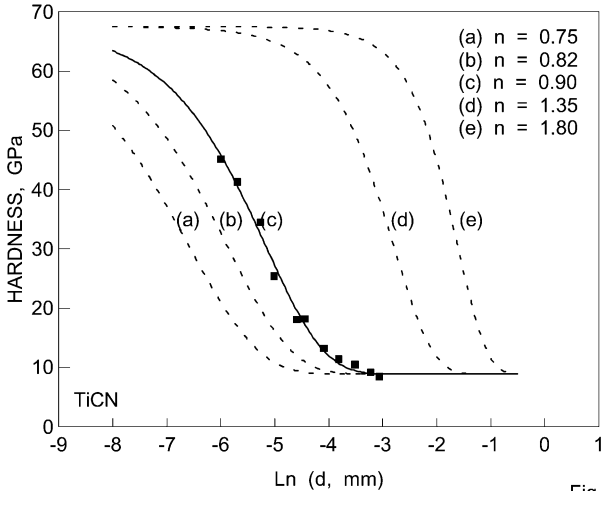

Fig. 15. Effect of the change in the parameter n in Eq. (12), on the displacement of the composite hardness of the TiCN curve. Both the film hardness and the parameter k have been kept constant.

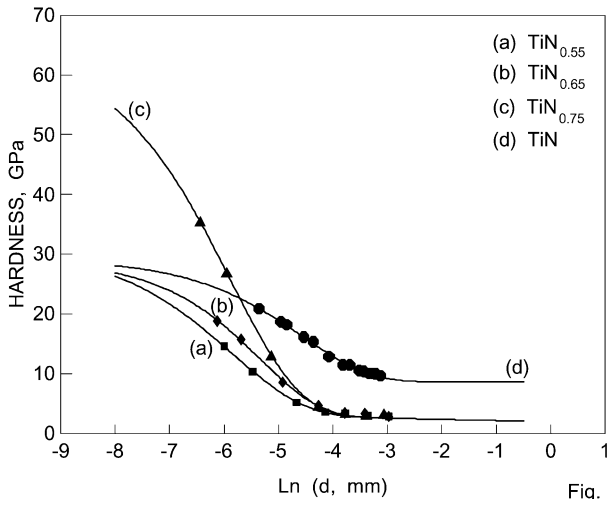

Fig. 16. Comparison of the composite hardness vs. ln of the indentation diagonal for the three under stoichiometric TiN_x films and the TiCN coating.

In relation to the physical meaning of the parameters k and n present in Eq. (12), Figs. 14 and 15 illustrate the effect in the change of any of these constants on the description of the experimental data for the particular case of the TiCN coating. Fig. 14 shows that as k decreases, keeping constant the values of H_C and n, the composite hardness curve is displaced towards the right of the plot while the rate of change of the composite hardness remains the same, indicating that the coating material is able to sustain its hardness to larger indentation loads.

On the other hand, in order to evaluate the effect of the parameter n and given the functional dependence between k and n indicated in Eq. (10), it would be better to re-write Eq. (12) as:

$$H = H_S + (H_C - H_S)\exp(-k' t_c^n Z_R^n)$$

Thus, Fig. 15 illustrates that as the parameter n increases, keeping constant the value of H_C and k', the curve is also displaced significantly towards the right of the plot and the transition in hardness is much more steep, indicating again that the film is able to sustain its properties to larger loads. Thus, it can be concluded that the best coatings, from the present point of view, would be those characterized by low k and large n values. On this basis it is possible to compare coatings of a similar hardness, from the standpoint of their nature, composition and deposition mode.

For example, Fig. 16 shows a comparison between the different TiN films analyzed in the present work, whereas Fig. 17 illustrates a comparison between the different ZrN coatings also investigated. In Fig. 16 it is clearly seen that as the nitrogen content of the under stoichiometric coatings increases the film hardness also increases. Since the substrate material was the same for the three coatings, it is observed that as the load applied increases the composite hardness tends to achieve the same final hardness. However, the rate of decrease appears to be higher for the $TiN_{0.75}$ coating than for the other two films. Regarding the stoichiometric coating, TiN, deposited on a tool steel, whose hardness is comparable to that of the $TiN_{0.65}$ film, it can be observed that the composite hardness curve is displaced towards the right of the $TiN_{0.65}$ coating. Thus, the hardness of the former is maintained to higher indentation loads, which indicates a coating of better properties as predicted from the value of the parameter k reported in Table 2. In relation to Fig. 17 relative to the ZrN coatings, it can also be observed that as the nitrogen content increases the film hardness also increases and that the rate of decrease in the composite hardness is more marked for the $ZrN_{0.70}$ film.

In both cases (TiN_x and ZrN_y films), the rate of decrease of the composite hardness is intimately related to the film hardness whose determination depends critically on the experimental values of the composite hardness. As it has already been shown, the modified model published by Tuck et al. [15] is a particular form of the more general model developed in the present communication and it tends to saturate at the predicted film hardness at low values of the relative indentation depth, earlier than predicted by Eq. (12). Thus, a relative disadvantage of both models is that in order to be fully tested, reliable nano indentation measurements would be required, such that the upper knee of the composite hardness curve could be defined without ambiguity.

A final comment regarding the present model is that, similarly to the other four models analyzed, an ISE could be easily included, by assuming that the film

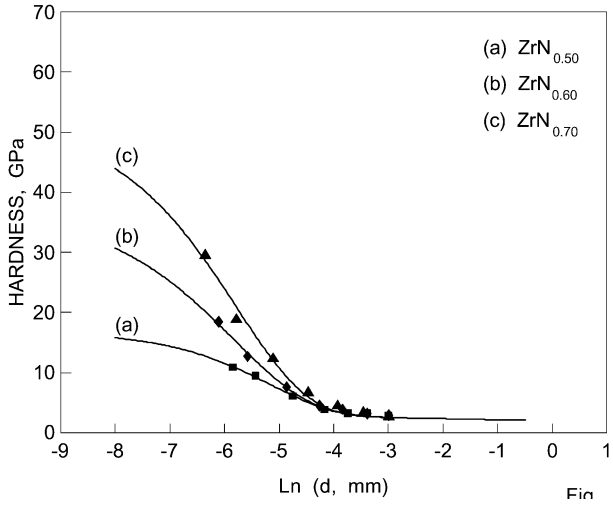

Fig. 17. Comparison of the composite hardness vs. ln of the indentation diagonal for the three under stoichiometric ZrN_x films.

hardness can be expressed as a function of the indentation diagonal by means of the models proposed either by Meyer [19] or Thomas [7]:

$$H_S = H_{0S} d^{p-2} \quad \text{or} \quad H_S = H_{0S} + \frac{b}{d}, \tag{20}$$

respectively. The above consideration and assuming the validity of Meyer's law [19], would transform Eq. (12), in an expression of the form:

$$H = H_S + (H_{0C} d^{p-2} - H_S)\exp(-kZ_R^n) \tag{21}$$

which would increase to four the number of parameters to be identified from the experimental data. However, these parameters could also be determined precisely by defining an objective function of the form:

$$\varphi = \sum_{i=1}^{N} \{H_i - H_S - (H_{0C} d_i^{p-2} - H_S)\exp(-kZ_{Ri}^n)\}^2; Z_{Ri} = \frac{d_i}{7t_c} \tag{22}$$

and solving the following system of equations:

$$\frac{\partial \varphi}{\partial H_{0C}} = 0; \quad \frac{\partial \varphi}{\partial p} = 0; \quad \frac{\partial \varphi}{\partial k} = 0; \quad \frac{\partial \varphi}{\partial n} = 0 \tag{23}$$

5. Conclusions

A simple model for the description of the composite hardness as a function of the indentation diagonal has been derived on a rational basis and from simple geometrical considerations. It has been shown that such a model is able to capture the most relevant characteristics of the complex dependence of the hardness of coated systems on the scale of indentation. Also, it has been shown that it is able to describe satisfactorily the hardness data obtained from different coated systems including Ti and TiC formed on a high-carbon chromium steel, CrN, TiN and TiCN deposited on a M2 steel and a number of under stoichiometric films of TiN_x and ZrN_y deposited on 316L stainless steel. It is believed that the model could be used satisfactorily for the description of coated systems in which the film thickness varies between approximately 1–4 μm, that is to say, the same range of coating thicknesses for which the other models reported in the literature are employed. It has been shown that the modification of the original model developed by Korsunsky et al. [13], put forward by Tuck et al. [17], constitutes a special form of the present model, although both approaches leads to different predictions regarding the parameters involved, including the film hardness. Similarly to the modified model published by Tuck et al., the present model provides two parameters that allow the evaluation of the coating performance in comparison with other coatings. As well as the other models analyzed in the present study, the model advanced can also be modified in order to incorporate the ISE of the film material through both the models proposed by Meyer and Thomas.

Acknowledgments

This investigation has been conducted with the financial support of the Venezuelan National Fund for Scientific and Technological Research (FONACIT) through the projects LAB-97000644 and S1-2000000642, and the Scientific and Humanistic Development Council of the Universidad Central de Venezuela through the project PG-08-17-4595-2000. The author gratefully acknowledges the collaboration of Dr Deepak Bhat for the provision of the CrN, TiN and TiCN data and to Dr Jonathan A. Berríos for the provision of the TiN_x and ZrN_y data.

References

[1] H. Bückle, in: J.W. Westbrook, H. Conrad (Eds.), The Science of Hardness Testing and its Research Applications, American Society for Materials, Metals Park, OH, 1973, p. 453.
[2] B. Jönsson, S. Hogmark, Thin Solid Films 114 (1984) 257.
[3] P.J. Burnett, T.F. Page, J. Mater. Sci. 19 (1984) 845.
[4] O. Vingsbo, S. Hogmark, B. Jönsson, A. Ingermarsson, Microindentation Techniques in Materials Science and Engineering, ASTM STP 889, ASTM, Philadelphia, PA, 1986, p. 257.
[5] P.J. Burnett, D.S. Rickerby, Thin Solid Films 148 (1987) 41.
[6] P.J. Burnett, D.S. Rickerby, Thin Solid Films 148 (1987) 51.
[7] A. Thomas, Surf. Eng. 3 (2) (1987) 117.
[8] S.J. Bull, D.S. Rickerby, Surf. Coat. Technol. 42 (1990) 149.
[9] P.A. Engel, A.R. Chitsaz, E.Y. Hsue, Thin Solid Films 207 (1992) 144.
[10] D. Chicot, J. Lesage, Thin Solid Films 254 (1995) 123.
[11] A. Iost, R. Bigot, Surf. Coat. Technol. 80 (1996) 117.
[12] F. Attar, Surf. Coat. Technol. 78 (1996) 78.
[13] A.M. Korsunsky, M.R. McGurk, S.J. Bull, T.F. Page, Surf. Coat. Technol. 99 (1998) 171.
[14] D. Chicot, Y. Bénarioua, J. Lesage, Thin Solid Films 359 (2000) 228.
[15] J.R. Tuck, A.M. Korsunsky, S.J. Bull, Surf. Coat. Technol. 127 (2000) 1.
[16] H. Ichimura, F.M. Rodriguez, A. Rodrigo, Surf. Coat. Technol. 127 (2000) 138.
[17] J.R. Tuck, A.M. Korsunsky, D.G. Bhat, S.J. Bull, Surf. Coat. Technol. 137 (2001) 217.
[18] E.S. Puchi-Cabrera, J.A. Berrios, D. Teer, Surf. Coat. Technol. 157 (2002) 183.
[19] D. Tabor, The Hardness of Metals, Clarendon Press, Oxford, 1951.